Quasi-analytical and rigorous modeling of interference microscopy

Tobias Pahl[1,*], *Johannes* Breidenbach[1], and *Peter* Lehmann[1]

[1]Measurement Technology Group, Faculty of Electrical Engineering and Computer Science, University of Kassel, Wilhelmshöher Allee 71, Kassel 34121, Germany

Abstract. We present an extended vectorial Kirchhoff model of coherence scanning interferometry including several vector rotations occurring in the imagining and scattering process as well as polarization dependent reflection coefficients. For validation simulated results are compared to those of the conventional scalar Kirchhoff model and a rigorous finite element modeling.

1 Introduction

Optical surface topography measurement techniques such as coherence scanning interferometry (CSI) are widespread for fast and contactless measurement of surface features with lateral dimensions of several 100 nm and an axial resolution down to the subnanometer range. However, due to the wave characteristics of light and resulting diffraction effects, optical profilers suffer from systematic deviations occurring in context with surface characteristics [1–3]. In order to predict and analyze these deviations, numerical models, which can be subdevided into quasi-analytic and rigorous models depending on the assumptions made in the computation of the scattering process, are being developed. Usually, quasi-analytic models require less computation time and memory. They provide better insight in physical mechanisms of the imaging and scattering process. On the other hand, rigorous simulations show higher accuracy since no rough approximations are made. In previous studies quasi-analytic models are developed based on Fourier optics or scalar Kirchhoff theory to analyze systematic deviations and the transfer characteristics of CSI systems [3–6]. However, if imaging systems of high numerical aperture (NA) are used, a vectorial mathematical treatment is essential. In [7] a vectorial extension of the scalar Kirchhoff model is presented. However, the model shows inconsistencies since the electric field is not anymore perpendicular to the wave vector after the scattering process.

This contribution presents an extension of the vectorial model, where inconsistencies are fixed and local reflection coefficients depending on the local surface slope are considered. For validation, results obtained from the vectorial model are compared to those of the scalar Kirchhoff theory and a rigorous finite element method (FEM) based model described in [8].

*e-mail: tobias.pahl@uni-kassel.de

2 Model

The models presented in this study consider a Linnik interferometer of high NA and single color LED illumination. Hence, the influence of temporal coherence is neglected. Further, scattering geometries are considered to be invariant under translation in one direction (here y) and apodization as well as aberrations are neglected for simplicity. In general, the interference intensity I_{int} is computed by

$$I_{\mathrm{int}}(x,z) \sim \int_0^{2\pi} \mathrm{d}\varphi_{\mathrm{in}} \int_0^{\theta_{\max}} \mathrm{d}\theta_{\mathrm{in}} I_{\mathrm{int};\theta_{\mathrm{in}},\varphi_{\mathrm{in}}}(x,z) \sin(\theta_{\mathrm{in}}) \cos(\theta_{\mathrm{in}}), \tag{1}$$

where θ_{in} is the incidence angle with respect to the optical (z-) axis, φ_{in} the azimuth angle and $I_{\mathrm{int};\theta_{\mathrm{in}},\varphi_{\mathrm{in}}}(x,z) \sim \mathrm{Re}\{\mathbf{E}_{\mathrm{o};\theta_{\mathrm{in}},\varphi_{\mathrm{in}}}(x,z) \cdot \mathbf{E}^*_{\mathrm{r};\theta_{\mathrm{in}},\varphi_{\mathrm{in}}}(x)\}$ the two-beam interference intensity with the electric fields $\mathbf{E}_{\mathrm{o/r}}$ of the object under investigation and the reference mirror, respectively [7]. The calculation of $\mathbf{E}_{\mathrm{o}}$ differs depending on the model.

2.1 Scalar Model

In the scalar model the electric field corresponds to a scalar field distribution $\psi_{\mathrm{o};\theta_{\mathrm{in}},\varphi_{\mathrm{in}}}$. Based on the Beckmann formulation of scattering [9], the field distribution scattered by a periodic phase object of height profile $h(x)$, amplitude ψ_0 and period length L_x is given by $\psi_{\mathrm{o};\theta_{\mathrm{in}},\varphi_{\mathrm{in}}}(x,z) = \psi_0 \mathrm{e}^{\mathrm{i}q_z(h(x)+z)}$, where $\mathbf{q} = (q_x, q_x, q_z)^T = \mathbf{k}_{\mathrm{s}} - \mathbf{k}_{\mathrm{in}}$ with the scattered and incident wave vectors $\mathbf{k}_{\mathrm{s/in}}$. Hence, the field in the image plane of a microscope obtained from the scattered field can be described by the Fourier series

$$\psi_{\mathrm{o};\theta_{\mathrm{in}},\varphi_{\mathrm{in}}}(x,z) = \sum_{n=n_{\min}}^{n_{\max}} \sqrt{\frac{k_{\mathrm{s};zn}}{k_{\mathrm{in};z}}} c_n \mathrm{e}^{\mathrm{i}2\pi n x/L_x - \mathrm{i}q_{z,n} z}, \tag{2}$$

where $n_{\min}$ and $n_{\max}$ are limited by the NA of the objective lenses, c_n is the Fourier coefficient [3] and the root term considers energy conservation.

2.2 Vectorial extension

If objective lenses of high NA are used, a vectorial treatment of the scattering process increases the accuracy of modeling. Therefore, the electric field is calculated by

$$\mathbf{E}_{\mathrm{o};\theta_{\mathrm{in}},\varphi_{\mathrm{in}}}(x,z) = \sum_{n=n_{\min}}^{n_{\max}} \underline{R}^{\mathrm{T}}(\theta_{\mathrm{s};n},\varphi_{\mathrm{s};n})\underline{T}(\theta_{\mathrm{s};n},\varphi_{\mathrm{s};n}) \sqrt{\frac{k_{\mathrm{s};zn}}{k_{\mathrm{in};z}}}\mathbf{c}_n \mathrm{e}^{\mathrm{i}2\pi n x/L_x - \mathrm{i}q_{z,n}z}, \quad (3)$$

where $\underline{T}$ represents a rotation matrix in x, z plane ensuring that the electric field remains perpendicular to the corresponding wave vector, $\underline{R}^{\mathrm{T}}$ describes the rotation of the scattered electric field passing the objective lens and

$$\mathbf{c}_n = \frac{1}{L_x}\int_{-L_x/2}^{L_x/2} \mathrm{d}x \mathrm{e}^{-\mathrm{i}q_z h(x)}\mathrm{e}^{-\mathrm{i}2\pi n x/L_x} \left[R_{\perp;\theta_{\mathrm{in}},\varphi_{\mathrm{in}}}(x)\mathbf{E}_{\mathrm{in},\perp;\theta_{\mathrm{in}},\varphi_{\mathrm{in}}}(x) + R_{\parallel;\theta_{\mathrm{in}},\varphi_{\mathrm{in}}}(x)\mathbf{E}_{\mathrm{in},\parallel;\theta_{\mathrm{in}},\varphi_{\mathrm{in}}}(x)\right] \quad (4)$$

is the 3D Fourier coefficient. The reflection coefficients $R_{\perp;\theta_{\mathrm{in}},\varphi_{\mathrm{in}}}$, $R_{\parallel;\theta_{\mathrm{in}},\varphi_{\mathrm{in}}}$ as well as the components $\mathbf{E}_{\mathrm{in},\perp;\theta_{\mathrm{in}},\varphi_{\mathrm{in}}}$, $\mathbf{E}_{\mathrm{in},\parallel;\theta_{\mathrm{in}},\varphi_{\mathrm{in}}}$ of the incident electric field $\mathbf{E}_{\mathrm{in};\theta_{\mathrm{in}},\varphi_{\mathrm{in}}}$ perpendicular and parallel to the plane defined by the incident wave vector and the surface normal $\mathbf{n}(x)$ vary with respect to the x axis due to the dependency of $\mathbf{n}$ on the surface slope. The incident electric field $\mathbf{E}_{\mathrm{in};\theta_{\mathrm{in}},\varphi_{\mathrm{in}}} = \underline{R}(\theta_{\mathrm{in}},\varphi_{\mathrm{in}})\mathbf{E}_0$ is given by the rotation of the initial electric field vector $\mathbf{E}_0$ by the rotation matrix $\underline{R}$ considering the rotation of the field being focused. The normal vector is calculated numerically based on the derivative of $h(x)$.

3 Results

Figure 1 shows interference signals obtained from a sinusoidal nickel surface profile with maximum surface slope of 18° and $L_x = 6\,\mu\mathrm{m}$ simulated with monochromatic illumination of wavelength $\lambda = 440\,\mathrm{nm}$ using the scalar model (a), the vectorial model (c) and the FEM model presented in [8] (e). In all three cases, the sinusoidal profile can be seen clearly in the course of the maximum interference intensity. For better comparability Figs. 1(b, d, f) show the interference signals in hybrid $x\,q_z$-space, where a band pass filtering behavior according to the surface slope is observed as explained and experimentally confirmed by Künne et al. [10]. Since FEM calculates the light scattering process rigorously, FEM results are used for reference. Comparing Figs. 1(b) and 1(d), the vectorial modeling shows a slight improvement of the models accuracy. However, having regard to surface profiles including steep surface slopes, multiple scattering and shadowing effects become more important leading to still significant deviations between quasi-analytic and rigorous modeling. Nonetheless, in order to analyze transfer characteristics of microscopic imaging systems usually analytical models are preferred and hence, the vectorial extension may improve the accuracy of quasi-analytical models.

4 Conclusion

A scalar Kirchhoff model is extended by a vectorial treatment, where several rotations of the electric field during the focusing and scattering processes are considered. Comparing results obtained by scalar and vectorial Kirchhoff modeling to rigorous FEM results, the vectorial modeling provides slightly different and more realistic results compared to the scalar modeling. Therefore, considering objective lenses of high NA and surfaces of certain characteristics, a vectorial treatment of the imaging and scattering process may be preferred in order to analyze the transfer behavior of CSI systems in future studies.

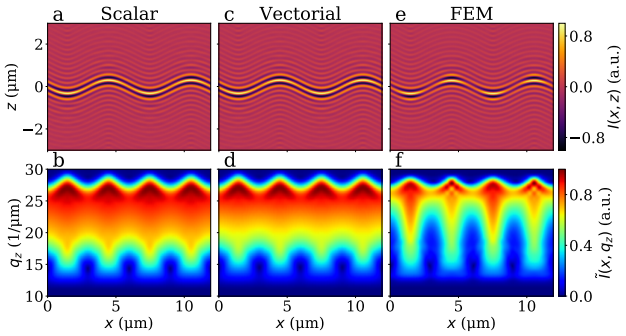

Figure 1: Offset reduced interference signals obtained from a sinusoidal surface profile with $L_x = 6\,\mu\mathrm{m}$ and maximum surface slope of 18° simulated with the scalar model (a), vectorial model (c) and FEM (e). The bottom row displays the Fourier transform of the interference intensities shown in the upper row with respect to the optical axis.

References

[1] A. Harasaki, J. Wyant, Applied Optics **39**, 2101 (2000)
[2] P. de Groot, X. Colonna de Lega, J. Kramer, M. Turzhitsky, Applied Optics **41**, 4571 (2002)
[3] W. Xie, P. Lehmann, J. Niehues, S. Terechenko, Optics Express **24**, 14283 (2016)
[4] P. de Groot, X. Colonna de Lega, JOSA A **37**, B1 (2020)
[5] R. Su, R. Leach, Light: Advanced Manufacturing **2**, 1 (2021)
[6] P. Lehmann, S. Hagemeier, T. Pahl, Metrology **1**, 122 (2021)
[7] T. Pahl, S. Hagemeier, M. Künne, C. Danzglock, N. Reinhold, R. Schulze, M. Siebert, P. Lehmann, Proc. SPIE **11783**, 117830G (2021)
[8] T. Pahl, S. Hagemeier, M. Künne, D. Yang, P. Lehmann, Optics Express **28**, 39807 (2020)
[9] P. Beckmann, A. Spizzichino, *The scattering of electromagnetic waves from rough surfaces* (Artech House, Inc., USA, 1987)
[10] M. Künne, T. Pahl, P. Lehmann, Proc. SPIE **11782**, 117820T (2021)